

# Instanton-noninstanton transition in nonintegrable tunneling processes: A renormalized perturbation approach

AKIRA SHUDO<sup>1 (a)</sup>, YASUTAKA HANADA<sup>1 (b)</sup>, TERUAKI OKUSHIMA<sup>2 (c)</sup> and KENSUKE S. IKEDA<sup>3 (d)</sup>

<sup>1</sup> *Department of Physics, Tokyo Metropolitan University, Minami-Osawa, Hachioji, Tokyo 192-0397, Japan*

<sup>2</sup> *Science and Technology Section, General Education Division, College of Engineering, Chubu University, Matsumoto-cho, Kasugai, Aichi 487-8501, Japan*

<sup>3</sup> *College of Science and Engineering, Ritsumeikan University Noji-higashi 1-1-1, Kusatsu 525, Japan*

PACS 05.45.Mt – Quantum chaos; semiclassical methods

PACS 05.45.-a – Nonlinear dynamics and chaos

PACS 03.65.-w – Quantum mechanics

**Abstract** – The instanton-noninstanton (I-NI) transition in the tunneling process, which has been numerically observed in classically nonintegrable quantum maps, can be described by a perturbation theory based on an integrable Hamiltonian renormalized so as to incorporate the integrable part of the map. The renormalized perturbation theory is successfully applied to the two quantum maps, the Hénon and standard maps. In spite of different nature of tunneling in the two systems, the I-NI transition exhibits very common characteristics. In particular, the manifestation of I-NI transition is obviously explained by a remarkable quenching of the renormalized transition matrix element. The enhancement of tunneling probability after the transition can be understood as a sudden change of the tunneling mechanism from the instanton to quite a different mechanism supported by classical flows just outside of the stable-unstable manifolds of the saddle on the top of the potential barrier.

Poincaré proved that almost all the classical Hamiltonian systems are nonintegrable. The tunneling process in classically integrable systems is described almost completely by the instanton theory and is understood in terms of classical trajectories [1]. However, the theory of tunneling in classically nonintegrable systems remains far from complete, and is still one of the unsolved fundamental problems in theoretical physics. It has been more than two decades since the study of nonintegrable tunneling starts [2–7] (see recent progress in [8, 9]). In the energy domain approach, the application of the Herring’s formula to nonintegrable systems [10, 11], hybrid approaches combining pure quantum and semiclassical theory, which was applied to explaining chaos-assisted tunneling [4, 12, 13] and resonance-assisted tunneling [2, 14], and so on have been proposed. On the other hand, in the time domain approach, the complex domain semiclassical theory has revealed a crucial role of the complexified stable-unstable

manifold mechanism, which implies the importance of Julia sets [15–17]. However, the relation and correspondence between theories and numerical investigations are not yet clear enough and there is no unified view.

Most of works have been devoted to the so-called quantum maps which model the essence of nonintegrable feature of quantum dynamics in a simple minded way. A very important result which has been reported in several works is that even a very weak nonintegrable perturbation leads to a remarkable enhancement of the tunneling rate [2, 13, 14, 18–21]. This transition is a common feature observed for quantum maps but its basic origin is still controversial and is not understood completely.

Wave functions of non-integrable systems are localized on classical tori in the nearly-integrable regime according to the well-known Einstein-Brillouin-Keller (EBK) quantization rule. A remarkable feature of the invariant torus in nonintegrable system is that it breaks at a border called the natural boundary on which singularities are densely accumulated [22].

It was conjectured that the natural boundary interrupts the instanton, thereby may influence the tunneling rate

(a) E-mail: shudo@tmu.ac.jp

(b) E-mail: hanada-yasutaka@ed.tmu.ac.jp

(c) Email: okushima@isc.chubu.ac.jp

(d) Email: ahoo@ike-dyn.ritsume.ac.jp

[8]. Indeed, clear evidence has been demonstrated recently manifesting that the remarkable enhancement of the tunneling rate is closely connected with the interruption of instanton due to the natural boundary [21]. We call the first transition from the instanton tunneling to some unknown type of tunneling as the instanton-noninstanton (I-NI) transition, which occurs in a notable manner in quantum maps. In the present paper, by introducing a perturbation theory based upon maximal renormalization of the integrable part, we show clearly that a different tunneling process supported by classical flow just outside of the stable-unstable manifolds of the saddle at the top of the potential barrier induces the transition to the NI regime.

In what follows, we take the symmetric form of the quantum map  $U = e^{-iP^2/4\hbar} e^{-i\epsilon V(Q)/\hbar} e^{-iP^2/4\hbar}$  (or  $U = e^{-i\epsilon V(Q)/2\hbar} e^{-iP^2/2\hbar} e^{-i\epsilon V(Q)/2\hbar}$ ). Redefining the effective Planck constant as  $\kappa = \hbar/\sqrt{\epsilon}$  and the new set of conjugate operators  $p = -i\kappa d/dq$  and  $q = Q$ , then  $U$  becomes a convenient form in our approach

$$U = e^{-i\sqrt{\epsilon}p^2/4\kappa} e^{-i\sqrt{\epsilon}V(q)/\kappa} e^{-i\sqrt{\epsilon}p^2/4\kappa}. \quad (1)$$

Figs. 1(a) and (b) are typical examples of tunneling characteristics computed for two typical quantum maps, namely the Hénon and standard maps. The figures show the representative tunneling probability as a function of the quantum number, and they exhibit a typical feature of the I-NI transition. Here the quantum maps have the potential functions  $V(Q) = 2Q^2 + Q^3/3$  (the Hénon map) and  $\cos Q$  (the standard map), respectively. Although these examples are nonintegrable, we here examine weakly nonintegrable regimes with small  $\epsilon$  as displayed in the insets of fig. 1. Therefore, the classical invariant tori still remain according to the celebrated Kolmogorov-Anold-Moser (KAM) theory, and good quantum numbers can be assigned to each quantum eigenstate following the EBK quantization rule.

In the limit of vanishing nonintegrability, both systems are approximated by one-dimensional systems with potential barriers which classically bound the eigenstates but quantum mechanically allow to tunnel by the instanton mechanism as is usual in one-dimensional systems, which will be discussed later. However, as the quantum number  $n$  decreases from the highest excited state with the energy just below the potential barrier height, a transition occurs at a characteristic quantum number, denoted hereafter by  $n_c$ , and the tunneling probability suddenly deviates from the instanton probability forming a *plateau*. The common feature seems to be quite paradoxical in the sense that the low lying states distant from the saddle point located on the barrier top, which is the very origin of the classical nonintegrability exhibit non-instanton tunneling, while the highly excited states close to the saddle point obey the instanton tunneling. Moreover, in both examples the number of the eigenstates in the instanton regime  $n_{\max} - n_c$  is insensitive to  $\hbar$ , where  $n_{\max}$  is the maximum quantum number of the classically bounded states inside

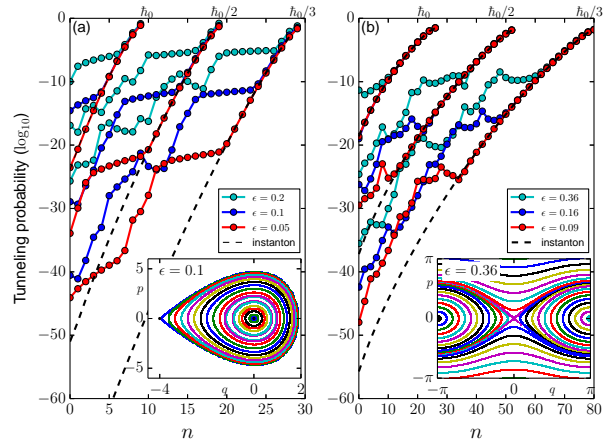


Fig. 1: The tunneling probability (in  $\log_{10}$ ) for the eigenstates of eq. (1) vs the quantum number  $n$  (less than  $n_{\max}$ ) for (a) the Hénon and (b) the standard map with various values of  $\hbar$  in the unit of  $\hbar_0$  and the nonlinear parameter  $\epsilon$ . The tunneling probability is computed in the asymptotic region ( $Q \ll -4$ ) for the Hénon map and at the the potential top ( $Q = 0$ ) for the standard map (only the even parity eigenfunctions in the  $q$ -representation are considered). Here  $\hbar_0 = 0.63\sqrt{\epsilon}$  for the Hénon map and  $\hbar_0 = \frac{3\pi}{25}\sqrt{\epsilon}$  for the standard map. Insets shows the phase space portrait of classical maps with  $\epsilon = 0.1$  and  $\epsilon = 0.36$  for the Hénon and standard maps, respectively.

the potential well.

To understand the I-NI transition the most natural way is to apply a perturbation theory based on an integrable limit which has the instanton as the tunneling mechanism. The crudest integrable approximation of symmetrized  $U$  in the small limit of the nonlinear parameter  $\epsilon$  is  $U_1 = e^{-i\sqrt{\epsilon}/\kappa H_1}$  where  $H_1 = p^2/2 + V(q)$ , but the difference  $|U - U_1| \sim \epsilon^2/\kappa$  is too large to afford any significant result for the exponentially small tunneling effect. We therefore develop a systematic expansion with respect to the smallness parameter  $\epsilon$  which renormalizes the integrable part of  $U$  into a single effective Hamiltonian as much as possible. A possible candidate to achieve this is the Baker-Hausdorff-Campbell (BHC) expansion, which approximates the product of exponential operators (1) systematically in terms of a single exponential operator expressed by an effective Hamiltonian, which coincides with  $H_1$  in the lowest-order approximation.

Below, we apply a renormalized perturbation theory to the Hénon and standard maps. They are both simplest classes of maps exhibiting quite different nature of tunneling, which is understood by the simplest one-dimensional Hamiltonian  $H_1 = p^2/2 + V(q)$ : the Hénon map has the cubic potential with the bottom at  $q = 0$  and tunneling is an irreversible transport of probability toward  $q = -\infty$  going over the barrier at  $q = -4$ . For the standard map the  $4\pi$  periodic boundary condition is imposed in the  $q$  direction. Then its cosine potential gives two symmetric valleys with bottoms at  $q = \pm\pi$  and separated by two symmetric

barriers at  $q = 0$  and  $q = 2\pi$ .

We can show that the BHC expansion of  $U$  leads to an effective polynomial Hamiltonian

$$H_{\text{eff}}^{(M)} = \sum_{\ell=1,3,\dots,M} (-\epsilon)^{(\ell-1)/2} H_\ell \quad (2)$$

with  $H_\ell = \sum_{k,i,j=0}^{k_\ell, i_{\ell k}, j_{\ell k}} \kappa^k C(\ell, k, i, j) p^i q^j$ ,

where  $C(n, k, i, j)$  is the set of coefficients of  $O(1)$ , and the terms of  $k = 0$  provide the classical Hamiltonian. Note that only the odd powers of  $\epsilon^{1/2}$  appear in the sum because of the symmetrized form of  $U$ . The unitary operator thus induced is given as  $U_M = e^{-i\sqrt{\epsilon}/\kappa H_{\text{eff}}^{(M)}}$ . We do not introduce any artificial absorbers and/or absorbing boundary conditions, which may crucially influence the original dynamics [13, 14].

Once the renormalized Hamiltonian is obtained, we straightforwardly develop a perturbation theory taking the difference  $\Delta U_M = U - U_M = O(\epsilon^{(M+1)} \sqrt{\epsilon}/\kappa)$  as the perturbation. Then the lowest-order perturbative eigenfunction is given as

$$\begin{aligned} |\Psi_n^{(M)}\rangle &= |u_n^{(M)}\rangle + |\Delta\Psi_n^{(M)}\rangle, \\ |\Delta\Psi_n^{(M)}\rangle &= \sum_j \frac{\langle u_j^{(M)} | \Delta U_M | u_n^{(M)} \rangle}{e^{-i\sqrt{\epsilon}/\kappa E_n^{(M)}} - e^{-i\sqrt{\epsilon}/\kappa E_j^{(M)}}} |u_j^{(M)}\rangle, \end{aligned} \quad (3)$$

where  $|u_n^{(M)}\rangle$  and  $E_n^{(M)}$  are respectively the eigenfunction and the energy eigenvalue of the 1D integrable Hamiltonian  $H_{\text{eff}}^{(M)}$ .

If  $\epsilon$  is not so large, there appear two sorts of fixed points in classical phase space: stable and unstable fixed point  $(0, 0)$  and  $(-4, 0)$  for the Hénon map, and  $(\pm\pi, 0)$  and  $(0, 0)$  for the standard map respectively. As shown in the insets of fig. 1, KAM tori predominate phase space in both cases and KAM regions are encircled by the stable manifold  $W^s$  and the unstable manifold  $W^u$  of the saddle fixed point. KAM tori support quantum eigenstates, each of which satisfies the EBK quantization condition  $\int pdq/2\pi = (n + 1/2)\kappa$  ( $n = 0, 1, \dots, n_{\text{max}}$ ). They all have finite tunneling life-times (Hénon map) or tunneling splittings (standard map) due to the tunneling via the instanton trajectory, which is very well approximated by the lowest order instanton solution  $p = \sqrt{2(V(q) - E_n)}$  or  $H_1(ip, q) = E_n$  ( $E_n$  is the quantized energy). A notable feature of the renormalized Hamiltonian  $H_{\text{eff}}^{(M)}(p, q)$  is that tunneling tails of eigenfunctions  $\langle q | u_n^{(M)} \rangle$  do not change very significantly even if one increases the order of renormalization  $M$ . However, according to eq.(3), the application of perturbation changes drastically the tunneling tail of eigenstates with increase in  $M$ .

In fig. 2(b) we show a typical result of renormalized perturbation theory. For lower-order approximation,  $U - U_M$  is too large to control correctly the exponentially small tunneling component and so the perturbative solution

yields quite absurd results. But as the order  $M$  of renormalization increases the perturbative solution converges to the exact eigenfunction  $|\Psi_n\rangle$  obtained by numerical diagonalization and reproduces even the complicated oscillations at the tunneling tail as demonstrated in figs. 2 (a1) and (a2). The higher-order renormalized perturbation calculation also succeeded in reproducing the exact tunneling probability in a rather wide regime including both I (instanton) and I-NI transition regions. (See figs. 2 (b1) and (b2)).

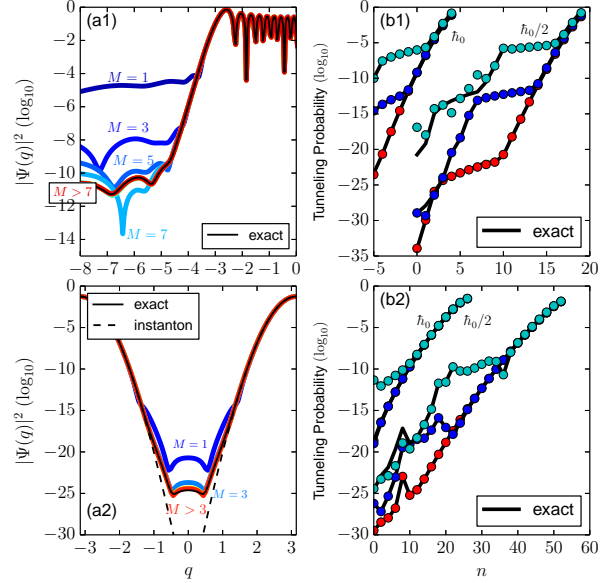


Fig. 2: The convergence of tunneling tail to the exact numerical one (black) with increase in  $M$  in case of (a1)  $n = 13$ -th excited state of the Hénon map with  $\epsilon = 0.1$  and  $h = h_0/2$ , and (a2) the ground state of standard map with  $\epsilon = 0.36$  and  $h = h_0/2$ . The exact and higher order renormalized perturbative results are not distinguishable with each other. Right-hand panels show the probability amplitude of tunneling tail of exact numerical diagonalization (black lines) and of perturbation calculation as a function of quantum number (less than  $n_{\text{max}}$ ) in case of (b1) the Hénon map with the order  $M = 21$ , and (b2) the standard map with the order  $M = 7$ . In (b2) the quantum number is shifted by  $-5$  for  $h_0$ , and so  $n = -5$  means  $n = 0$  for  $h_0$ .

The success of the perturbation theory means that the origin of the I-NI transition may be resolved into integrable bases: according to eq. (3) we define the *contribution spectrum* representing the amount of contribution from the  $j$ -th eigenstate of the integrable model to the  $n$ -th perturbative eigenfunction:

$$\begin{aligned} \text{Con}_{j \rightarrow n}^{(M)} &\equiv \langle\langle | \langle q | u_j^{(M)} \rangle | \rangle \rangle | \langle u_j^{(M)} | \Psi_n^{(M)} \rangle | \simeq \\ &\begin{cases} \langle\langle | \langle q | u_j^{(M)} \rangle | \rangle \rangle | \langle u_j | \Delta \Psi_n^{(M)} \rangle | & (\text{if } j \neq n) \\ \langle\langle | \langle q | u_n^{(M)} \rangle | \rangle \rangle & (\text{if } j = n) \end{cases} \end{aligned} \quad (4)$$

where  $\langle\langle \dots \rangle\rangle$  means to take average over a range of  $q$  in the

asymptotic region (Hénon map) or around  $q = 0$  (standard map).

We discuss closely how the renormalized perturbation theory describes the I-NI transition by taking the contribution spectrum of the Hénon map as an example. Figure 3(a) shows how the contribution spectrum  $\text{Con}_{j \rightarrow n}^{(M)}$  ( $0 \leq j \leq n_{\max}$ ) varies with the order of renormalization  $M$  at two representative quantum numbers  $n$  before and after the I-NI transition. A quite interesting fact is that for  $M = 1$  the largest contribution comes from a broad peak centered at  $j = n^*$ , where  $n^*$  is the number of a quantum state just above the threshold of dissociation  $n = n_{\max}$ . However, with increase in the renormalization order  $M$ , the transition matrix elements  $|\langle u_j^{(M)} | \Delta U_M | u_n^{(M)} \rangle|$  are remarkably quenched, and the peak at  $j = n^*$  is reduced in the logarithmic scale and finally overwhelmed by the very sharp peak at  $j = n$ , which means that the contribution from instanton of the integrable basis  $\langle q | u_n^{(M)} \rangle$  is predominant in the tunneling process. On the other hand, at  $n$  less than a critical quantum number  $n_c$  the quenching of the transition matrix element can no longer reduce the peak at  $j = n^*$  less than the instanton peak, and the contribution to tunneling is attributed to the broad peak around  $j = n^*$ . The competition between the two peaks explains the characteristics of I-NI transition. It should be emphasized that without remarkable quenching of the transition matrix element by renormalization the instanton phase is absent and the I-NI transition cannot be observed.

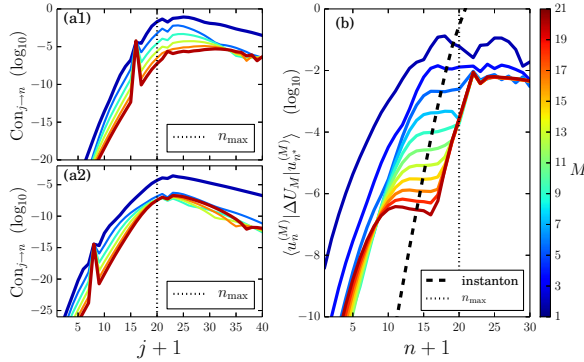


Fig. 3: Typical contribution spectra  $\text{Con}_{j \rightarrow n}^{(M)}$  of (a1) before and (a2) after the I-NI transition. (a1) and (a2) respectively correspond to  $n = 15$  and  $n = 7$  of the Hénon map with  $\epsilon = 0.1$  and  $\hbar = \hbar_0/2$  (see fig. 2(b1)). The renormalization order grows as  $M = 1, 5, 9, 13, 17, 21$ . (b) The major transition matrix element  $|\langle u_n^{(M)} | \Delta U_M | u_{n^*}^{(M)} \rangle|$  vs  $n$  for the same Hénon map, where  $n^* = 21 = n_{\max} + 2$ .  $M$  is increased from 1 to 21. The black dotted curve denotes the instanton peak amplitude  $\langle \langle q | u_n^{(M)} \rangle \rangle$  of the  $n$ -th state. The vertical axis is drawn in the  $\log_{10}$  scale.

Since the above threshold state  $|u_{n^*}^{(M)}\rangle$  is connected with  $q = -\infty$  by real classical paths,  $|\langle q | u_{n^*}^{(M)} \rangle| \sim O(1)$  and so the peak strength  $\text{Con}_{n^* \rightarrow n}^{(M)}$  at  $n^*$  is approximated by the transition matrix element  $|\langle u_n^{(M)} | \Delta U_M | u_{n^*}^{(M)} \rangle|$ . Figure 3

(b) plots  $|\langle u_n^{(M)} | \Delta U_M | u_{n^*}^{(M)} \rangle|$  at just above the threshold for various values of  $M$ . The instanton peak strength  $\langle \langle q | u_n^{(M)} \rangle \rangle$  is also shown as a function of  $n$ , which does not significantly depend on  $M$  as mentioned above.

With increase in  $M$ , the curve  $|\langle u_n^{(M)} | \Delta U_M | u_{n^*}^{(M)} \rangle|$  vs  $n$  is largely deformed to show a very characteristic structure: it decreases steeply as  $n$  decreases below  $n_{\max}$ , but it reaches a definite plateau and then it decreases again steeply. It is just on the plateau that the curve  $|\langle u_n^{(M)} | \Delta U_M | u_{n^*}^{(M)} \rangle|$  vs  $n$  intersects with the instanton peak curve, which means that tunneling using the transition to the state  $n = n^*$  overwhelms the instanton tunneling and so the intersection determines  $n_c$ . As  $M$  increases, the height of plateau decreases rapidly and reaches finally to a limit, which causes the instanton region  $n_c < n < n_{\max}$  to grow from a null region to a finite region with the width proportional to  $\sqrt{\epsilon}$ . Below  $n_c$ , the transition matrix element controls tunneling and so the tunneling probability follows the plateau structure, which explains the characteristic plateau of the tunneling amplitude seen in fig.2.

The origin of the transition to a plateau-like characteristics of the tunneling rate from the instanton tunneling rate reported in preceding works can therefore be attributed to the formation of the plateau of the transition matrix element and a drastic decrease of plateau height in higher-order renormalization. The I-NI transition in the standard map in fig.1(b) follows the same scenario [23].

We note that if one shifts each curve in Fig. 1 horizontally such that the maximal quantum number  $n_{\max}$  for each curve coincides with each other, they all show very similar characteristics, and are insensitive to the effective Planck constant  $\kappa$ . Such a feature can hardly be explained by classical objects *e.g.*, nonlinear classical resonances, which will be discussed in detail in our forthcoming papers [23].

Finally, we elucidate the classical dynamical significance of the plateau region which is characteristic after the I-NI transition. The above analyses tell us that the states composed of the self-component  $j = n$  and the ones forming the broad peak around  $j = n^*$  play as the principal component. We define here the principal component contributing to tunneling (PCT) and observe the phase space Husimplot to investigate the classical interpretation for the I-NI transition. The PCT is defined as the projection of  $|\Psi_n^{(M)}\rangle$  onto the principally contributing subspace constructed as follows. Let  $|u_j^{(M)}\rangle$  be eigenfunctions rearranged in descending order of the magnitude  $\text{Con}_{j \rightarrow n}$  in the contribution spectrum, and consider the  $K$ -dimensional subspace spanned by  $|u_j^{(M)}\rangle$  ( $1 \leq j \leq K$ ). Let  $K_{\min}$  be the minimum number of  $K$  which makes the relative distance between the vector  $|\Psi_n^{(M)}\rangle$  and its projection onto the above introduced subspace less than a small enough threshold value  $r_{th}$  ( $\ll 1$ ), namely, the minimal  $K = K_{\min}$  such that

$$\left\langle \left\langle \frac{|\langle q | \Psi_n^{(M)} \rangle - \sum_{j=0}^K \langle q | u_j^{(M)} \rangle \langle u_j^{(M)} | \Psi_n^{(M)} \rangle|}{|\langle q | \Psi_n^{(M)} \rangle|} \right\rangle \right\rangle < r_{th}$$



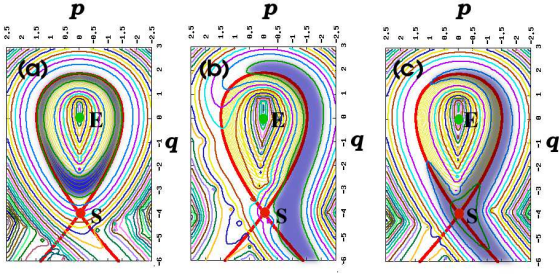


Fig. 4: Husimi plots of the PTC for the eigenfunctions of the Hénon map with  $\epsilon = 0.10$  and  $\hbar = \hbar_0/2$  (see fig. 2(b1)). (a) before ( $n = 15$ ), and (b) after ( $n = 13$ ) the I-NI transition, and (c) is the eigenstate at the edge of plateau ( $n = 7$ ). (a) and (c) correspond to fig. 3(a1) and (a2), respectively. Contours are plotted in log scale, and the shaded regions indicates the highest levels. The red curve is the  $W^s$ - $W^u$  complex of the saddle  $S$  (red circle), and the green dot  $E$  denotes the stable fixed point. The Husimi levels of (a) coincide entirely with the eigenfunction of  $|u_{15}^{(M)}\rangle$  of  $H_{\text{eff}}^{(M)}$ , which has its major body inside of the  $W^s$ - $W^u$  complex, while in (b) and (c) the major body winds around  $W^s$ , passes nearly to  $S$  and is blown to  $-\infty$  following the  $W^u$ . The maximum level of contour is  $10^{0.5}$  in (a), suddenly drops to  $10^{-4.5}$  in (b) after the I-NI transition

Then the space spanned by  $|u_j^{(M)}\rangle$  ( $1 \leq j < K_{\min}$ ) constitutes the principally contributing subspace to tunneling. We take  $r_{th} = 0.2$ , for example. We have to emphasize that  $M$  must be taken sufficiently large ( $M \geq 13$  in practice) in order that the PCT is significant.

The Husimi plots of the PCT before and after the I-NI transition are depicted in fig. 4. The shadowed region indicates the region with the highest probability level. In the instanton regime the PCT coincides almost with the eigenfunction  $|u_n^{(M)}\rangle$  of the unperturbed integrable Hamiltonian, and the Husimi plot of PCT in fig. 4(a) indeed traces the classical invariant circle shown as the shadowed region, and the tunneling component is represented by the monotonously decaying contours encircling the shaded quantized invariant circle. In particular, when observed in the  $q$ -coordinate, the tunneling tail is the line  $p = 0$  passing across the saddle  $S$ , which is nothing more than the instanton.

On the other hand, fig. 4(b) indicates that a drastic change occurs in PCT when the transition to NI happens: the main component, characterized by almost the same probability levels, runs along the stable manifold  $W^s$ , attracted and repelled by the saddle  $S$ , finally runs away toward  $q = -\infty$  along the unstable manifold  $W^u$ , which manifests that the PCT contributing to the tunneling tail represents classical flows just outside of the  $W^s$ - $W^u$  complex. The PCTs for all the eigenstates forming the plateau take almost similar patterns but they approach more closely to the  $W^s$ - $W^u$  complex, as the quantum number shifts to the edge of the plateau. Figure 4(c) shows that just at the eigenstate on the edge of the plateau its PCT coin-

cides with the  $W^s$ - $W^u$  complex. As is seen in fig. 1, the tunneling amplitude decreases rapidly when  $n$  is less than the plateau edge quantum number. All the above features are common in the Hénon and standard maps, which are more completely discussed in [23].

In the present paper we have developed a perturbation theory for nearly integrable quantum maps. This is based upon an integrable Hamiltonian which is constructed by maximally renormalizing the integrable part of the map. This was successfully applied to investigate the I-NI transition commonly observed in nearly integrable quantum maps such as the Hénon and standard maps. A remarkable quenching of the highly renormalized transition matrix elements explains the origin of the abrupt change of tunneling characteristics at the I-NI transition. The PCT analysis reveals that the tunneling mechanism in the plateau region after the I-NI transition is due to the classical flow outside of the  $W^s$ - $W^u$  complex is responsible for the tunneling process after the transition and the flow coincides with the  $W^s$ - $W^u$  complex at the edge of the plateau. This suggests the crucial role of classical dynamics related to the  $W^s$ - $W^u$  complex, and elucidating the relation to the complex stable-unstable manifolds mechanism based on the complex-domain semiclassics is strongly desired.

\*\*\*

Discussions with Y. Shimizu, K. Takahashi, A. Bäcker, R. Ketzmerick, N. Mertig and A. Mouchet are appreciated. This work was supported by Kakenhi 24340094 based on the tax of Japanese people, and the authors would like to acknowledge them. This was also supported by Chubu University Grant (26IIS06AII). The authors are very grateful to Shoji Tsuji and Kankikai for using their facilities at Kawaraya during this study.

## REFERENCES

- [1] SCHULMAN L. S., *Techniques and Applications of Path Integration* (Wiley-interscience) 1996.
- [2] BRODIER O., SCHLAGHECK P. and ULLMO D., *Phys. Rev. Lett.*, **87** (2001) 064101; *Ann. Phys.*, **300** (2002) 88. The effect of classical nonlinear resonances on tunneling was discussed in OZORIO DE ALMEIDA A. M., *J. Phys. Chem.*, **88** (1984) 6139.
- [3] LIN W. A. and BALLENTINE L. E., *Phys. Rev. Lett.*, **65** (1990) 2927.
- [4] BOHIGAS O., TOMSOVIC S. and ULLMO D., *Phys. Rep.*, **223** (1993) 45.
- [5] TOMSOVIC S. and ULLMO D., *Phys. Rev. E*, **50** (1994) 145.
- [6] HENSINGER W. K. *et al.*, *Nature*, **412** (2001) 52.
- [7] STECK D. A., OSKAY W. H. and RAIZEN M. G., *Science*, **293** (2001) 274.
- [8] CREAGH S. C., *Tunneling in Complex Systems*, edited by S. TOMSOVIC (Singapore, World Scientific) 1998, p. 35
- [9] *Dynamical Tunneling: Theory and Experiment*, edited by KESHAVAMURTHY S. and SCHLAGHECK P. (CRC Press) 2011.

- [10] WILKINSON M., *Physica D*, **21** (1986) 341.
- [11] CREAGH S. C. and FINN M. D., *J. Phys. A*, **34** (2001) 3792.
- [12] PODOLSKIY V. A. and NARIMANOV E. E., *Phys. Rev. Lett.*, **91** (2003) 263601.
- [13] BÄCKER A., KETZMERICK R., LÖCK S., and SCHILLING L., *Phys. Rev. Lett.*, **100** (2008) 104101; BÄCKER A., KETZMERICK R., and LÖCK S., *Phys. Rev. E*, **82** (2010) 056208.
- [14] LÖCK S., BÄCKER A., KETZMERICK R. and SCHLAGHECK P., *Phys. Rev. Lett.*, **104** (2010) 114101.
- [15] SHUDO A. and IKEDA K. S., *Phys. Rev. Lett.*, **74** (1995) 682; *Physica D*, **115** (1998) 234.
- [16] SHUDO A., ISHII Y. and IKEDA K. S., *J. Phys. A*, **42** (2009) 265101; **42** (2009) 265102.
- [17] TAKAHASHI K. and IKEDA K. S., *J. Phys. A*, **43** (2010) 192001.
- [18] RONCAGLIA, R., BONCI, L., IZRAILEV, F.M., WEST, B. J. and GRIGOLINI, P., *Phys. Rev. Lett.*, **73** (1994) 802.
- [19] SHEINMAN M., FISHMAN S., GUARNERI I. and REBUZZINI L., *Phys. Rev A*, **73** (2006) 052110.
- [20] MOUCHET A., *J. Phys. A*, **40** (2007) F663.
- [21] SHUDO A. and IKEDA K. S., *Phys. Rev. Lett.*, **109** (2012) 154102.
- [22] GREENE M. and PERCIVAL I. C., *Physica*, **3D** (1981) 530.
- [23] HANADA Y., SHUDO A. and IKEDA K. S., in preparation; SHUDO A., HANADA Y., OKUSHIMA T. and IKEDA K. S., in preparation.